Adsorption 4, 35–56 (1998)

Adsorption of the Ternary Liquid Mixture Ethanol/*n*-Octane/*n*-Hexadecane onto Activated Carbon: I. The Adsorption Excess of the Ternary Mixture and of Its Binary Combinations

G. KALIES, U. MESSOW, P. BRÄUER AND K. QUITZSCH
Institute of Physical and Theoretical Chemistry, University of Leipzig, Linnéstr. 2, 04103 Leipzig, Germany

Received October 2, 1996; Revised December 4, 1996; Accepted April 8, 1997

Abstract. The adsorption isotherms of the binary mixtures of ethanol/*n*-Octane, ethanol/*n*-hexadecane and *n*-octane/*n*-hexadecane onto the activated carbon TA 95 were measured at 278 K, 288 K, 298 K and 308 K and described with mathematical functions. About 300 experimental values of the adsorption excess of the ternary mixture ethanol/*n*-octane/*n*-hexadecane onto activated carbon TA 95 at 298 K were measured by gas chromatography inside the ternary triangle. The ternary miscibility gap was determined at three temperatures. A good representation of the ternary data and the calculated activity coefficients (using the UNIFAC model) in three-dimensional space was possible with the help of transformation of coordinates. It was possible, too, by utilization of the conception of the quasi two-component representation of the mole fractions with and without miscibility gap. Several influencing factors on ternary adsorption isotherms were discussed for the system ethanol/*n*-octane/*n*-hexadecane/TA 95.

Keywords: liquid phase adsorption, binary and ternary mixtures, excess isotherms, miscibility gap, mathematical description

Introduction

Separation and purification of liquid mixtures by adsorption have become very important in chemical industry. In spite of the growing interest in energy-saving adsorption onto solids from multicomponent liquid mixtures a relatively small number of publications concerning adsorption from three- and multicomponent mixtures covering the whole concentration range have been published (e.g., Goworek et al., 1985; Jaroniec and Madey, 1988; Borowko and Rzysko, 1995).

This situation is well-founded by some factors influencing the research progress:

1. The experimental expenditure for the determination of ternary or higher-order adsorption excess is high. On the other side literature reveals many experimental data for adsorption of binary liquid mixtures for a variety of adsorbents because of the good measurement possibilities (e.g., Groszek, 1970; Ozawa et al., 1984; Messow et al., 1992).
2. Predictions of adsorption in ternary and higher-order mixtures using experimental data on adsorption from binary mixtures have been only successful in the past, if the analytical equations fitting the data were simple.
3. Most experimental and theoretical studies have been concerned with adsorption from dilute solutions.
4. In the common understanding of ternary data the Gibbs triangle is the basis of the spatial arrangement. There the excess adsorption is often represented in the form of isolines in the plane (Goworek and Kusak, 1989). These representations permit a discussion of adsorption effects, but offer no mathematical or physical function, which describes the experimental data. Despite the rapid development of data processing the graphical representation of ternary data in the four-dimensional space remains difficult. Often the conception of the quasi two-component representation of the mole fractions is used for three-dimensional representations (Goworek, 1991). These representations in form

of $y = f(x_3, C)$, where $C = x_2/(x_1 + x_2)$, offer advantages for the treatment of thermodynamical equations, but it is difficult to think in this kind of representation. It would be better to create a representation in form of $y = f(x_1, x_2, x_3)$ with the basis of a Gibbs triangle.

5. The mathematical description of the measured ternary excess data is of great interest for the calculation of the specific free wetting energy and further for the calculation of the wetting enthalpy and the wetting entropy from the temperature dependence of the adsorption excess. Especially in a system with a miscibility gap it is complicated to find suitable functions to fit the experimental data.

In this paper experimental results of adsorption of the ternary mixture *n*-hexadecane/*n*-octane/ethanol and the binary mixtures belonging to it onto activated carbon are represented. The relatively complicated real ternary adsorption system is characterised through size and shape differences of the adsorbate molecules. With the two ideal components *n*-hexadecane and *n*-octane there are two *n*-paraffins of different chain length, whereas with ethanol there is a nonideal component in the mixture. In the case of activated carbon the adsorbent is nearly chemical homogeneous, so that the heterogeneity is limited to the surface and textural properties.

The purpose of this publication is a discussion of the ternary experimental data, a good display of the measured data in various graphical representations, which allow a deeper physico-chemical understanding and a mathematical description of the ternary adsorption excess as a basis of the thermodynamic treatment, even in the case of a system with miscibility gap.

Theory

Excess properties Y^σ are generally described by the Gibbs equation (Gibbs, 1931).

A common quantity for the description of liquid phase adsorption is the adsorption excess, related to the amount of substance. It is given by the experimentally accessible values according to

$$\Gamma_i^\sigma = \frac{n_i^\sigma}{m_A} = \frac{n^0\left(x_i^0 - x_i^l\right)}{m_A}; \quad i = 1, 2, 3, \ldots, \qquad (1)$$

Γ_i^σ = adsorption excess of component i related to the mass m_A of the adsorbent,
n^0 = total amount of substances of bulk and adsorption phase,
m_A = mass of adsorbent,
$x_i^0 - x_i^l$ = difference between the mole fraction of the considered component i before and after adsorption,
n_i^σ = excess amount of component i,

where

$$\Gamma_1^\sigma + \Gamma_2^\sigma + \Gamma_3^\sigma + \cdots = 0. \qquad (2)$$

The aim of the thermodynamic treatment is the calculation of immersion quantities, for example the immersion entropy and immersion enthalpy from adsorption isotherms in order to compare them with direct measured quantities (Bräuer et al., 1998). The central quantity for the calculations is the specific free wetting energy or the so-called surface pressure. Similar to the derivation of the binary specific free wetting energy (compare Heuchel et al., 1989; Bräuer et al., 1993) the derivation of the ternary specific free wetting energy from the fundamental equation of the excess formalism and the Gibbs-Duhem-equation is possible.

It is evident that the representation of the thermodynamic functions is convenient as a function of the variables $C = x_2/(x_1 + x_2)$ and x_3 (Goworek, 1991).

The line $C = \text{const.}$ can be considered as a pseudo component and corresponds to a straight line between a point D on the triangle bottom and a point A in the triangle top of Fig. 1. In this way we consider a pseudo two-component mixture.

The specific free wetting energy is given by

$$\Phi(x_3, C) - \Phi^{12}\left(x_2^{12}, x_3 = 0\right) = -RT \int_{x_3=0}^{x_3} A\, dx_3 \qquad (3)$$

with

$$\begin{aligned} A = {} & \frac{\Gamma_3^\sigma}{x_3(1 - x_3)} \\ & + \Gamma_2^\sigma \frac{1}{1 - C}\left[\frac{\partial \ln f_2}{\partial x_3} + \frac{x_3}{1 - x_3}\frac{\partial \ln f_3}{\partial x_3}\right] && (4) \\ & + \Gamma_3^\sigma \frac{C}{1 - C}\left[\frac{\partial \ln f_2}{\partial x_3} + \frac{1 - C(1 - x_3)}{C(1 - x_3)}\frac{\partial \ln f_3}{\partial x_3}\right], && (5) \end{aligned}$$

where Φ^{12} is the specific free wetting energy of the binary mixture (1, 2) and x_2^{12} is the mole fraction of

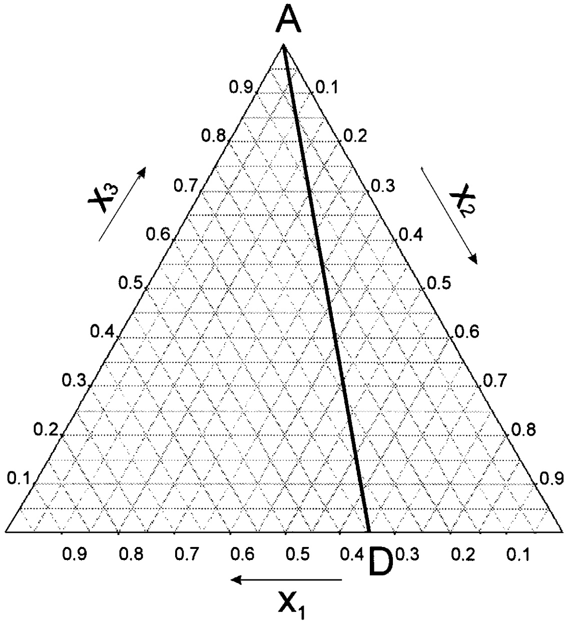

Figure 1. The way of integration to determine the specific free wetting enthalpy.

this binary mixture. f_i is the activity coefficient of the component i. Thus the wetting enthalpy can be calculated from adsorption isotherms of ternary adsorbed mixtures using the equation

$$\Delta h_{\mathrm{sp}}^{\sigma} - \Delta h_{\mathrm{sp}}^{\sigma,12} = \left\{\frac{[\partial(\Phi - \Phi^{12})/T]}{\partial(1/T)}\right\}_{p,x_3,C} \qquad (6)$$

except the constant $\Delta h_{\mathrm{sp}}^{\sigma,12}$. Therefore the immersion enthalpies of the binary system (1, 2) are necessary for a comparison between the calorimetrically measured immersion enthalpies of the ternary system and the calculated ones from adsorption excess isotherms.

Experimental

Materials

After some investigations with several carbonaceous adsorbents, especially Ambersorb adsorbents (Kalies et al., 1997), the activated carbon TA 95 (PICA), which was characterized by nitrogen adsorption (ASAP 2002 micropore system, 77.2 K), was used for the measurements. TA 95 combines a great BET-surface of 1585 m^2/g with an average pore diameter of about 8 Å, calculated using the micropore method (Mikhail et al., 1968) or the density function theory, respectively.

The elemental composition of TA 95 was determined by elemental analysis and is given by: H: 0.63%, N: 0.00%, S: 0.10%, O: 4.99%, Cl: 0.00%.

The adsorptives ethanol absolute (99.8%, MERCK), *n*-octane (99+%, ALDRICH) and *n*-hexadecane p.a. (stored over molecular sieve) were used without further purification.

Adsorption Isotherms

The measurements of binary adsorption isotherms were carried out with the three binary mixtures ethanol/*n*-hexadecane, ethanol/*n*-octane and *n*-octane/*n*-hexadecane onto TA 95 at 278 K, 288 K, 298 K and 308 K. The precision of temperature is ±0.3 K. TA 95 was activated 6 h at the temperature of 453 K before adsorption. All experiments were executed in glass tubes with screwings and teflon seals. A known weight of carbon (about 0.6 g) was introduced into about 2 g binary mixture of known concentration. The tubes were covered and stoppered in a water bath at the desired temperature. 50 μl in the case of refractometric analysis or 0.5 μl in the case of gas-chromatographic analysis of the exceeding solution were then removed for the purpose of analysis by drawing it through a microliter syringe. In this way, errors due to evaporation could be kept small. As a rule, the new concentration x_i^l of binary or ternary mixture over the adsorbent was determined after 24 h with Abbé- refractometry or gas chromatography (Perkin Elmer autosystem GC), respectively.

Ternary adsorption isotherms were measured for the system *n*-hexadecane/*n*-octane/ethanol/TA95 at 298 K. The Gibbs triangle is described by about 300 ternary points inside the triangle, about 80 binary points and about 20 points on the binodal curve. Each composition of the mixture before and after adsorption is reproduced at least by three gas chromatograms.

Ternary and Binary Miscibility Gap

The phase separation of the binary mixture ethanol/*n*-hexadecane was observed in dependence on temperature in a thermostat of the corporate LAUDA. About 10 ternary mixtures of known concentrations inside the miscibility gap of ethanol/*n*-octane/*n*-hexadecane were prepared. The concentrations of the components in the two phases were determined by gas chromatograpy after the phase separation at 289.65 K (this temperature is the lower limit because of the freezing point of *n*-hexadecane), 298.15 K and 308.15 K. Each composition of the mixture is reproduced at least by three gas chromatograms. Then about 0.6 g of the degassed adsorbent TA 95 were introduced into about 2 g ternary mixture at 298 K. For a period of half an hour a ‘wild’ mixing of the two phases (like a homogenization) occurred upon addition of the adsorbent. The adsorption systems were shake from time to time. After 24 hours the new concentrations of the components in the two phases were determined by gas chromatography after the phase separation.

Results and Discussion

Binary Adsorption Isotherms

Binary adsorption of a mixture ethanol/*n*-alkane or *n*-alkane/*n*-alkane onto carbonaceous adsorbents has often been described in literature (e.g., Findenegg, 1971; Everett, 1978; Kern and Findenegg, 1980; Ozawa et al., 1984; Kalies et al., 1995). Therefore the discussion of the binary adsorption phenomena will be restricted in this paper to a few facts.

The isotherm for the adsorption equilibrium of ethanol/*n*-octane onto the activated carbon TA 95 at 298 K is illustrated in Fig. 2. The shape of the excess isotherm corresponds to type 5 in the Schay and Nagy classification. In accordance to the real properties of the liquid phase *n*-octane is preferentially adsorbed at mole fractions until 0.62 of *n*-octane. Thereafter, ethanol is preferentially adsorbed. Ozawa et al. (1984) investigated adsorption of ethanol/*n*-heptane onto activated charcoal and found a similar adsorption behaviour (adsorption azeotrope at mole fraction of *n*-heptane $= 0.65$). The temperature dependence of the adsorption of ethanol/*n*-octane onto TA 95 is very low, if not negligible.

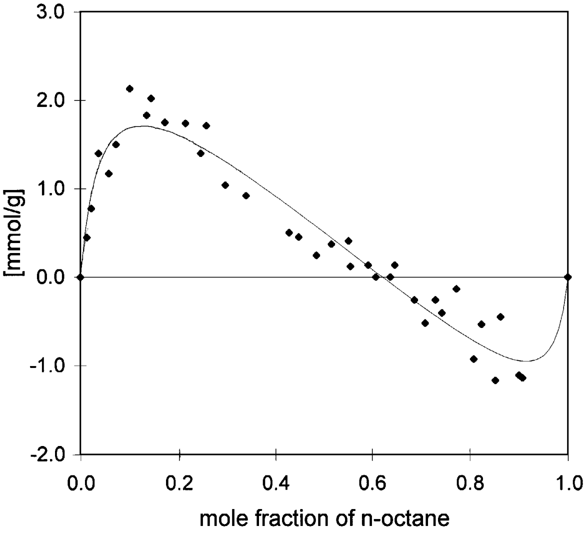

Figure 2. Adsorption of ethanol/*n*-octane onto TA 95 at 298 K described by a Bi-Langmuir function.

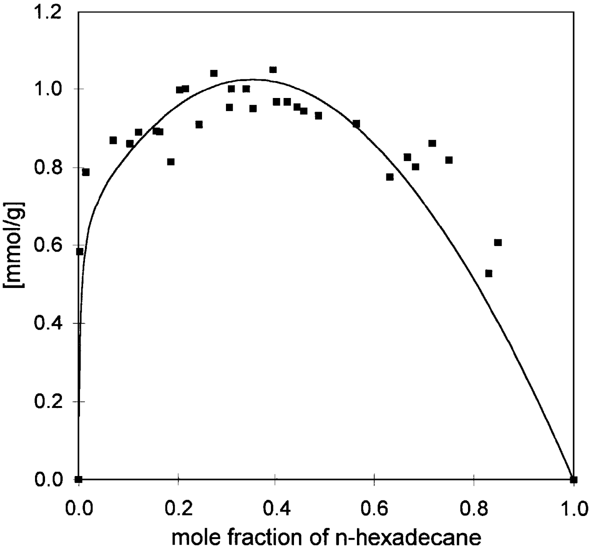

Figure 3. Adsorption of *n*-octane/*n*-hexadecane onto TA 95 at 298 K described by a Bi-Langmuir function.

The excess isotherm for the system *n*-octane/*n*-hexadecane/TA 95 at 298 K described by the Bi-Langmuir function is shown in Fig. 3. Carbonaceous adsorbents adsorb preferentially the long-chain *n*-alkanes (Kern and Findenegg, 1980). Despite a shift of the adsorption maximum in the *n*-octane direction, the isotherm corresponds to type 1 in the Schay and Nagy classification. Both components in the binary mixture show an almost ideal behaviour in bulk and adsorption phase. The small shift in the *n*-octane direction characterizes the relative high separation factor.

The isotherm for the system ethanol/*n*-hexadecane/TA 95 at 298 K in the initial concentration range of *n*-hexadecane shows a strong preferential adsorption of *n*-hexadecane. On the other hand a small preferential adsorption of ethanol could be established in the end of the concentration range of *n*-hexadecane (compare Fig. 4). The binary measurements of ethanol concentrations in this area were very difficult as a result of the very small amounts of ethanol. There is a danger of evaporation of ethanol during the refractometric

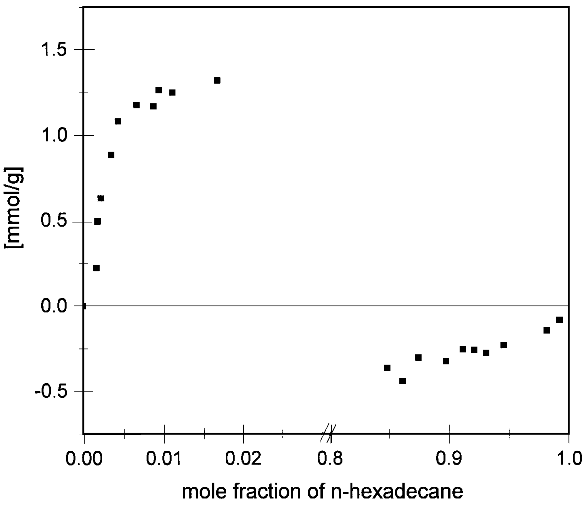

Figure 4. Adsorption of ethanol/*n*-hexadecane onto TA 95 at 298 K.

Table 1. Bi-Langmuir and Redlich-Kister parameters for binary adsorption of ethanol/*n*-octane, *n*-octane/*n*-hexadecane and ethanol/*n*-hexadecane onto TA 95 at 278, 288, 298 and 308 K.

	308 K	298 K	288 K	278 K
Bi-Langmuir parameter		Ethanol-*n*-octane		
Γ_m^s	6.02500	4.86641	6.28272	5.75884
h_A	0.64935	0.61768	0.62646	0.63938
U_A	7.20723	7.79460	6.93817	7.18443
U_B	−15.42023	−8.32208	−7.09535	−5.77863
Sum of mean-square errors	3.46817	1.85987	2.02217	1.49144
Bi-Langmuir parameter		*n*-Octane-*n*-hexadecane		
Γ_m^s	1.89238	13.29375	7.98729	4.79847
h_A	0.25740	0.04901	0.08247	0.15188
U_A	6.73606	18.12402	18.62837	13.81682
U_B	1.34972	0.50483	0.93666	1.24960
Sum of mean-square errors	0.25775	0.56121	0.29956	0.05751
Bi-Langmuir parameter		Ethanol-*n*-hexadecane		
Γ_m^s	5.38526	6.23144	6.98798	
h_A	0.50624	0.29518	0.32724	
U_A	13.39733	13.50916	12.13953	
U_B	−2.80532	−2.26044	−2.44058	
Sum of mean-square errors	0.39974	0.12573	0.29962	
Redlich-Kister parameter		Ethanol-*n*-octane		
A	2.37005	1.64557	1.92345	2.46470
B	−16.05224	−12.56517	−14.10100	−13.29900
C	3.54820	6.19710	9.97038	9.99970
Sum of mean-square errors	9.69390	6.02242	5.99828	6.12555
Redlich-Kister parameter		*n*-Octane-*n*-hexadecane		
A	1.46449	3.41690	3.94140	8.87730
B	−0.67070	−1.26910	−1.59930	21.73600
C	2.14450	6.01980	5.26910	28.52100
Sum of mean-square errors	0.23640	0.98075	1.11240	0.58046
Redlich-Kister parameter		Ethanol-*n*-hexadecane		
A	18.33900	22.99200	−152.65000	
B	−109.38000	−61.96300	−65.32500	
C	104.20000	35.75100	236.54000	
Sum of mean-square errors	1.64500	1.32817	1.27189	

analysis or the injection in the gas chromatograph and thus a danger of ethanol adsorption simulation.

The polynomial of Redlich and Kister with three parameters and the Bi-Langmuir function were used for the description of the excess isotherms. In the first case the polynomial was restricted to three parameters, because the polynomial with more parameters begins to swing. The resulting parameters of optimization and the sum of mean-square errors belonging to them are given in Table 1. To examine the resulting isotherm a combination of an efficient integration procedure named Runge-Kutta-Fehlberg (Forsythe et al., 1977) and of an algorithm developed by Nagel and Wolff for nonlinear parameter optimization (based on the Levenberg-Marquardt algorithm) was used. Using the program OPAL (Moros and Kalies, 1992) the differences between measured (exp) and calculated (calc) values were minimized by parameter optimization (Moros et al., 1996).

Utilizing the Bi-Langmuir function (Heuchel et al., 1986):

$$\Gamma_2^\sigma = \Gamma_m^s\left(x_2^s - x_2\right)$$

$$x_2^s = h_A \frac{K_A x}{1 + K_A x} + h_B \frac{K_B x}{1 + K_B x} \qquad (7)$$

$$x = \frac{x_2}{x_1}; \quad K_i = \exp\frac{\Delta U_i}{(RT)}; \qquad i = A, B$$

with

Γ_m^s = saturation amount of adsorption (mmol/g),

h_A = probability of adsorption sites of type $A \perp (h_A + h_B = 1)$,
U_A, U_B = difference of adsorption energies of component 1 and 2 with the types A and B of adsorption sites in kJ/mol: $U_A = U_{A2} - U_{A1}$, $U_B = U_{B2} - U_{B1}$,

the accordance between the measured and the calculated isotherm points is better than in the case of using the Redlich-Kister polynomial with three parameters (compare the sum of mean square errors in Table 1).

On the other hand, a physical interpretation is often not possible, because the calculated parameters are depending on the starting points of optimization. Therefore, the Bi-Langmuir equation is only used here as an analytical representation to smooth our experimental data.

Binary and Ternary Miscibility Gap

The measured points of the ethanol/*n*-hexadecane miscibility gap are illustrated and compared with the data points of Dahlmann and Schneider in Fig. 5 (Dahlmann and Schneider, 1989). Our measurements were carried out in the whole available temperature range to know exactly the beginning of the phase separation at 289.65 K, 298.15 K and 313.15 K. The Dahlmann and Schneider data in the higher temperature range underlay our data to a half Kelvin.

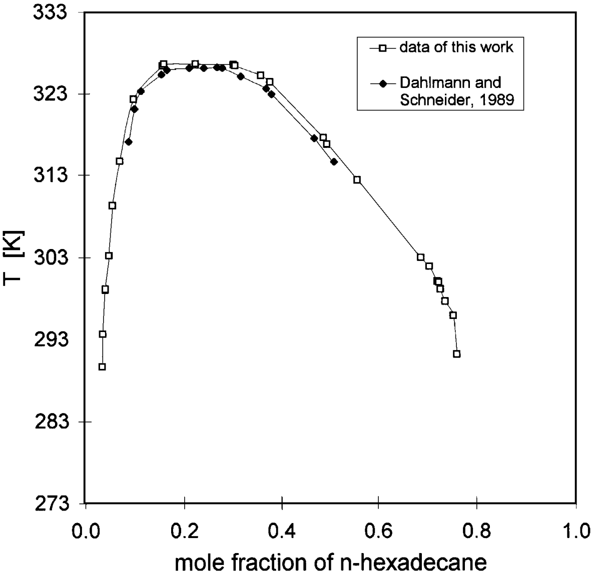

Figure 5. Binary miscibility gap of the mixture ethanol/*n*-hexadecane.

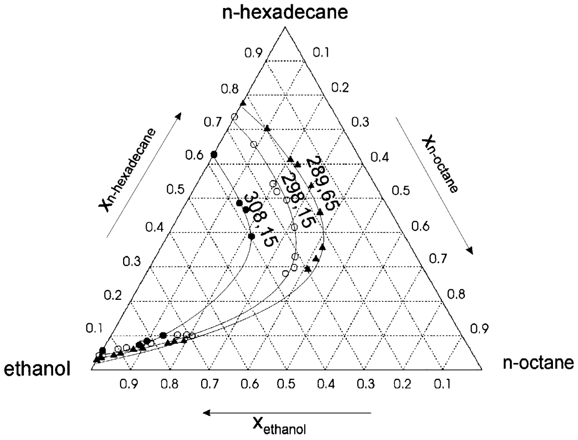

Figure 6. Temperature dependence for the miscibility gap of the mixture ethanol/*n*-octane/*n*-hexadecane.

The ternary miscibility gap of ethanol/*n*-octane/*n*-hexadecane at 289.65 K, 298.15 K and 308 K is shown in Fig. 6.

Point M which is characterizing a global composition of mixture and the coexisting phases α and β are lying on the tie-line (connode). The quantitative proportion of the coexisting phases is given by the so-called lever law of tie-lines:

$$\frac{\overline{M\alpha}}{\overline{M\beta}} = \frac{m_\beta}{m_\alpha} \tag{8}$$

with

$\overline{M\beta}, \overline{M\alpha}$ = distance between the point M and the point characterising the phase β for α,
m_β, m_α = mass of the phase β or α.

To calculate the adsorption excess on the binodal curve the following quantities are known:

— the amount of substances of bulk and adsorption phase: $n^0 = n_1^0 + n_2^0 + n_3^0$,
— the mole fraction of phase α: $x_i^{\alpha,0}$, $x_i^{\alpha,l}$, $i = 1, 2, 3$,
— the mole fraction of phase β: $x_i^{\beta,0}$, $x_i^{\beta,l}$, $i = 1, 2, 3$,

before or after adsorption, respectively.

It is also valid:

$$n^\alpha = n_1^\alpha + n_2^\alpha + n_3^\alpha$$

$$n^\beta = n_1^\beta + n_2^\beta + n_3^\beta$$

$$n^0 = n^\alpha + n^\beta.$$

The adsorption excess in phase χ is given by

$$\Gamma_i^{\sigma\chi} = \frac{\left(x_i^{\chi,\text{before}} - x_i^{\chi,\text{after}}\right) n_i^{\chi}}{m_A^{\chi}} \quad \text{with} \quad \chi = \alpha, \beta. \tag{9}$$

The mole fractions of the components in phase α and β before and after adsorption are known. It was necessary to calculate the amount of substance of component i in phase χ. An exact calculation of the distances $\overline{M\beta}$, $\overline{M\alpha}$ was possible through modifications in the program 4D Print (Reuter, 1995). Thus the calculation of the mass of the coexisting phases was possible and n_i^{χ} could be calculated.

Now the adsorbent mass remained the unknown quantity. If there is a model for the estimation of the adsorbent mass which takes “all alone” the responsibility for the adsorption excess in one phase then the adsorption excess of phase χ on the binodal curve is calculable. Although the adsorbent had only a direct contact with the lower phase after the phase separation (in our case the n-hexadecane-poor phase), the adsorbent mass weighed in was in connection with both phases because of the phase equilibrium. Therefore, it is difficult to separate the part of adsorbent m_A^{χ}, which is only responsible for the adsorption excess in one phase.

Examining different models for the determination of the adsorbent mass m_A^{χ} the adsorption mass m_A^{α} and m_A^{β} were calculated. In conclusion, it could be established that the following model of the mass calculation leads to a good accordance with measured ternary data out of the miscibility gap:

$$\frac{m_A^{\alpha}}{m_A^{\beta}} = \frac{n^{\alpha}}{n^{\beta}} \tag{10}$$

with

m_A^{χ} = adsorbent mass responsible for the adsorption in the phase χ,
n^{χ} = amount of substance in the phase χ.

In this way a description of all borders of the ternary excess triangle with a miscibility gap was given. The calcu’;ted binodal excess data onto TA 95 are included in all representations of the ternary adsorption excess data (see Figs. 7–11), as well as in all mathematical calculations.

Ternary Adsorption Isotherms

The position of binary and ternary data points is illustrated in Fig. 7 for the example of ternary adsorption of ethanol onto TA 95 (the data point number of the three components in mixture is something different because of the varying binary measure points). During the measurements it was tried to ‘go the way’ between the point D and the point A in Fig. 1, but beside the inaccuracy of the weighed-in quantities the adsorption process entails, of course, a positional shift.

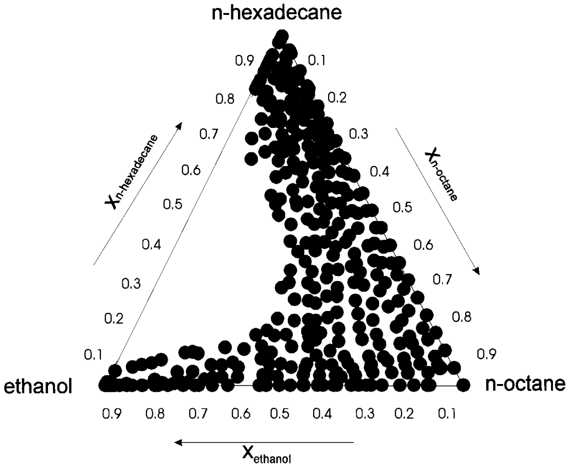

Figure 7. Position of measured ternary and binary adsorption excess data of ethanol onto TA 95 at 298 K, represented in the form $y = f(x_1, x_2, x_3)$.

The measured data records are of the form $\Gamma_{\text{ethanol}}^{\sigma} = f(x_1, x_2, x_3)$, $\Gamma_{n\text{-octane}}^{\sigma} = f(x_1, x_2, x_3)$ and $\Gamma_{n\text{-hexadecane}}^{\sigma} = f(x_1, x_2, x_3)$. All measured binary and ternany adsorption excess data are summarized in Table 3.

The component x_3 will be n-hexadecane, whereas ethanol will be x_1 and n-octane x_2. A substitution of x_1 and x_2 through C results in the three-dimensional representation $y = f(x_3, C)$ after Goworek. It is difficult to think in this kind of representation, because one top of the triangle (in our case n-hexadecane) is diverged to the side $C = 1$ of the quadratic representation.

The miscibility gap is described by a polynomial of 4th order in Fig. 8. To create a representation in form of $y = f(x_1, x_2, x_3)$ with the basis of a Gibbs triangle it is necessary to convert (x_1, x_2, x_3) into (x_0, y_0) in the following way:

$$\begin{aligned} (y_0)^2 &= (x_3)^2 - \left(\frac{x_3}{2}\right)^2 \\ y_0 &= \frac{\sqrt{3}}{2} x_3 \\ x_0 &= \frac{x_3}{2} + x_2. \end{aligned} \tag{11}$$

Now a mathematical description of the data was necessary. At first the kriging with a linear variogram, a

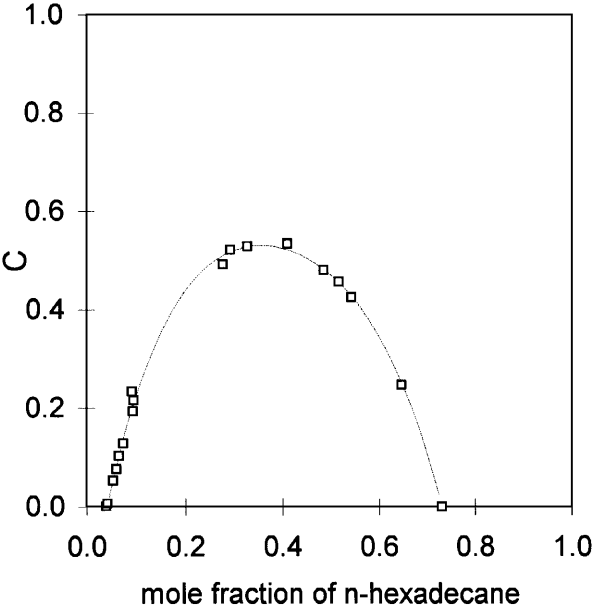

Figure 8. Ternary miscibility gap of ethanol/n-octane/n-hexadecane at 298 K described by a polynomial of 4th order, represented in the form $y = f(x_3, C)$.

geostatistical gridding method, was used to interpolate the data points. Kriging without a nugget effect is a so-called exact interpolator. These interpolators honor data points exactly if the data point coincides with the grid node being interpolated. With data sets of moderate size like our data sets with around 400 data points the kriging produces good data representations (Surfer for Windows, 1994).

In Fig. 9 the krigings of the ethanol adsorption are shown in the quadratic and the triangle representation. A comparison with a polynomial interpolation for the ethanol adsorption data set is given in Fig. 10. The polynomial regression is a smoothing interpolation and defines only the trend of the data. After some computations, polynomials of 6th order were used for the mathematical description of the data files because of the smallest mean-square error. The parameters of polynomials of 5th and 6th order for the data sets $\Gamma^{\sigma}_{\text{ethanol}} = f(x_3, C)$, $\Gamma^{\sigma}_{n\text{-octane}} = f(x_3, C)$, $\Gamma^{\sigma}_{n\text{-hexadecane}} = f(x_3, C)$ and $\Gamma^{\sigma}_{\text{ethanol}} = f(x_0, y_0)$, $\Gamma^{\sigma}_{n\text{-octane}} = f(x_0, y_0)$, $\Gamma^{\sigma}_{n\text{-hexadecane}} = f(x_0, y_0)$ are given in Table 2. The agreement between measured and calculated data is better in the case of the triangle representation as a result of the higher data density in the smaller triangle area. The data gaps entail a bad interpolation in this area, especially near the side $C = 1$ in the representation $y = f(x_3, C)$.

Now the measured ternary data are to be discussed.

The Gibbs triangle for the ternary ethanol adsorption is given in Fig. 10(b), the Gibbs triangles for the ternary n-octane and n-hexadecane adsorption are illustrated in Figs. 11(a) and (b). The same gray zones correspond to the same excess intervals. Looking at the ethanol adsorption in Fig. 10(b), the very high negative excess values of ethanol are remarkable in the ethanol rich corner of the triangle. The preferential binary adsorption of n-hexadecane as well as n-octane leads to an addition of the adsorption effects. Only in this corner below the miscibility gap the adsorption excess of ethanol is negative. The binary adsorption azeotrope (compare Fig. 2) of ethanol/n-octane at $x_{n\text{-octane}} \approx 0.62$ marks the beginning of the ternary adsorption azeotrope, which is shifting in the ethanol rich direction with increasing of the n-hexadecane concentration. The beginning of the ternary adsorption azeotrope at $x_{n\text{-octane}} \approx 0.62$ is an indication for a good

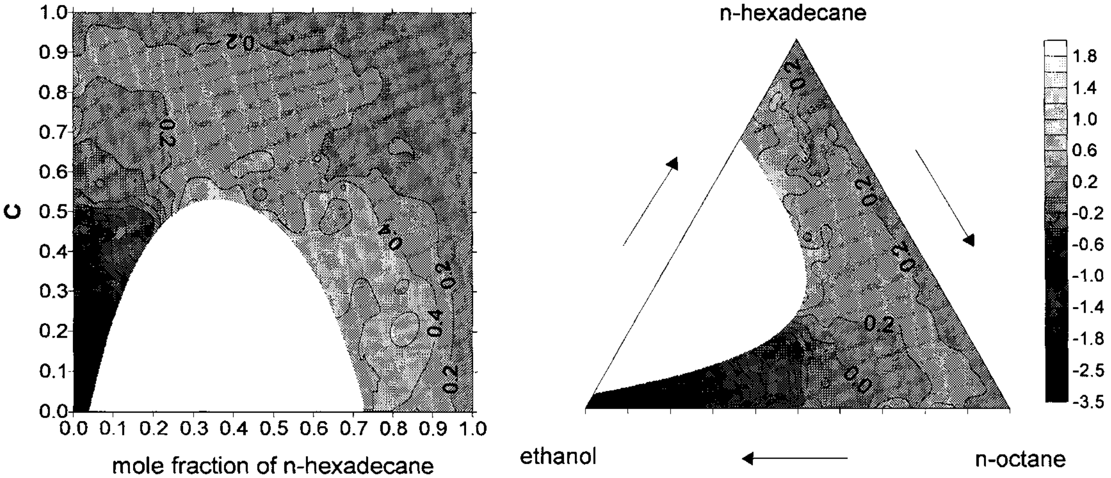

Figure 9. Krigings for ternary ethanol adsorption onto TA 95 at 298 K represented in the form: (a) $y = f(x_3, C)$ and (b) $y = f(x_1, x_2, x_3)$.

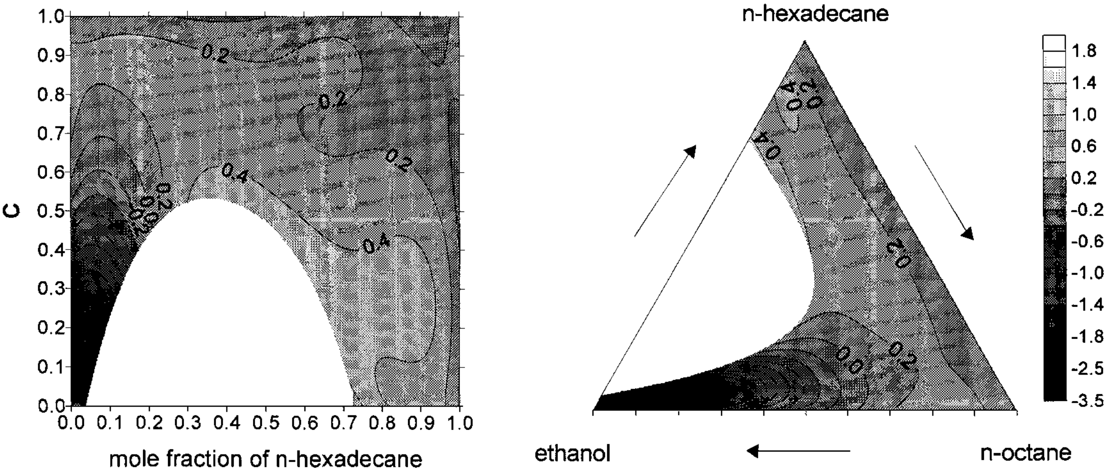

Figure 10. Polynomials of 6th order for ternary ethanol adsorption onto TA 95 at 298 K represented in the form: (a) $y = f(x_3, C)$ and (b) $y = f(x_1, x_2, x_3)$.

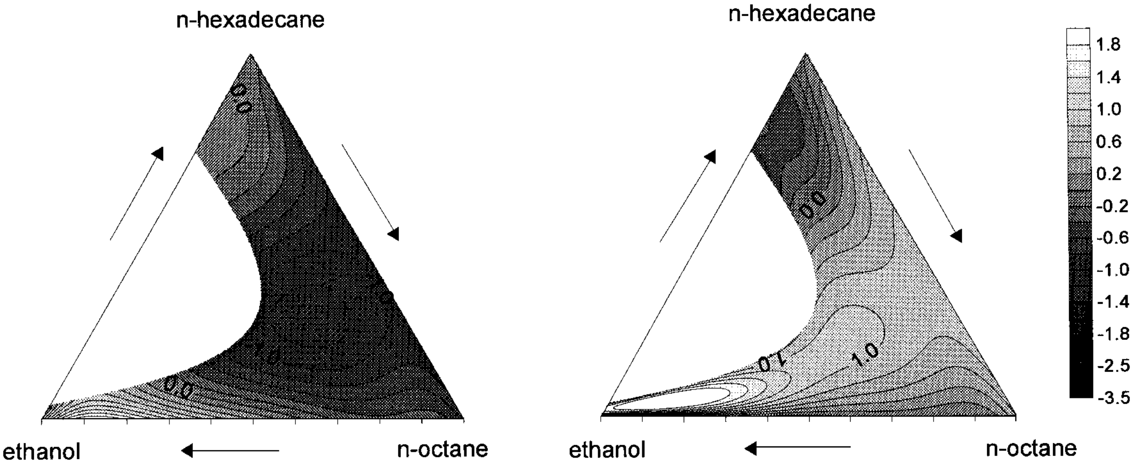

Figure 11. Polynomials of 6th order for ternary *n*-octane adsorption (a) and *n*-hexadecane adsorption (b) onto TA 95 at 298 K represented in the form $y = (x_1, x_2, x_3)$.

data description by the polynomial. It is easy to understand that the adsorption excess of ethanol is zero on the binary side *n*-octane/*n*-hexadecane.

In the remaining concentration range ethanol is a little enriched in the adsorption phase (values about 0.2). Caused by an interruption of the associate formation, which is probably on the average of third order, ethanol is adsorbed more preferentially. This result is confirmed by many published papers about binary solutions of alcohols in aliphatic hydrocarbons (e.g., Saris et al., 1986). The increasing of the ethanol excess on values greater than 0.4 in the high concentration range of *n*-hexadecane is interesting. It is conceivable that the long-chain alkane *n*-hexadecane disturbs stronger the ethanol association than *n*-octane and in this way ethanol will be adsorbed more preferentially. But at the same time the measurements of ethanol concentrations in this area were very difficult as a result of the very small amounts of ethanol (the mole fraction of ethanol is higher than the really weighed-in mass because of the different molar weights of the adsorptives) and the corresponding high vapour pressure of ethanol. There is a danger of evaporation of ethanol during the injection in the gas chromatograph.

Comparing the *n*-octane and *n*-hexadecane adsorption in Figs. 11(a) and (b), a nearly opposite adsorption excess is to be seen in the "*n*-octane half of the triangle" (the area between the points $x_{n\text{-octane}} = 0.5$, $x_{n\text{-octane}} = 1$ and $x_{n\text{-hexadecane}} = 1$). It is not surprising because of the small ethanol excess values in this area (Fig. 10(b)). The adsorption excess of *n*-octane is negative and *n*-hexadecane is positive. The

Table 2. Polynomials of 5th and 6th order for ternary adsorption of ethanol/*n*-octane/*n*-hexadecane onto TA 95 at 298 K.

Ethanol

Polynomial of 5th order for the triangle representation of the ternary ethanol adsorption onto TA 95 at 298 K:

$$\begin{aligned}z(x,y) = {} & -1.10239 - 6.25883y + 660.413y^2 - 1288.06y^3 + 877.04y^4 - 202.689y^5 - 24.6993x - 154.357xy + -1749.41xy^2 \\ & + 2443.38xy^3 - 843.095xy^4 + 144.845x^2 + 536.287x^2y + 1528.43x^2y^2 - 1176.09x^2y^3 - 295.275x^3 - 582.705x^3y \\ & - 436.071x^3y^2 + 267.003x^4 + 203.983x^4y - 90.7922x^5.\end{aligned}$$

Polynomial of 6th order for the triangle representation of the ternary ethanol adsorption onto TA 95 at 298 K:

$$\begin{aligned}z(x,y) = {} & -0.887888 - 85.576y + 3413.5y^2 - 8175.34y^3 + 7344.35y^4 - 2959.84y^5 + 452.428y^6 - 31.8046x - 279.556xy \\ & - 14191.1xy^2 + 27516.4xy^3 - 16656.8xy^4 + 3324.22xy^5 + 233.616x^2 + 2487.79x^2y + 21588.1x^2y^2 - 31086.1x^2y^3 \\ & + 9628.4x^2y^4 - 668.957x^3 - 4991.46x^3y - 13843.3x^3y^2 + 11615.5x^3y^3 + 960.621x^4 + 4010.34x^4y + 3027.44x^4y^2 \\ & - 681.658x^5 - 1138.96x^5y + 189.035x^6.\end{aligned}$$

Polynomial of 5th order for the quadratic Goworek representation of the ternary ethanol adsorption onto TA 95 at 298 K:

$$\begin{aligned}z(x,y) = {} & -1.17632 - 21.093y + 111.278y^2 - 200.181y^3 + 161.013y^4 - 49.7216y^5 - 1.48373x + 25.0403xy - 104.562xy^2 \\ & + 120.211xy^3 - 42.1311xy^4 + 48.4366x^2 - 31.1818x^2y + 23.3804x^2y^2 - 17.013x^2y^3 - 117.564x^3 + 48.3538x^3y \\ & + 0.425295x^3y^2 + 105.39x^4 - 23.9843x^4y - 33.5803x^5\end{aligned}$$

Polynomial of 6th order for the quadratic Goworek representation of the ternary ethanol adsorption onto TA 95 at 298 K:

$$\begin{aligned}z(x,y) = {} & -1.14271 - 23.5743y + 134.642y^2 - 269.138y^3 + 251.006y^4 - 104.015y^5 + 12.2074y^6 - 6.12106x + 5.27247xy \\ & - 126.978xy^2 + 302.701xy^3 - 230.754xy^4 + 57.2423xy^5 + 203.42x^2 - 152.526x^2y - 74.4056x^2y^2 - 23.4897x^2y^3 \\ & + 44.0609x^2y^4 - 670.405x^3 + 656.396x^3y + 29.5795x^3y^2 - 47.7212x^3y^3 + 838.883x^4 - 752.756x^4y + 45.5335x^4y^2 \\ & - 434.627x^5 + 266.852x^5y + 69.9728x^6.\end{aligned}$$

n-Octane

Polynomial of 5th order for the triangle representation of the ternary *n*-octane adsorption onto TA 95 at 298 K:

$$\begin{aligned}z(x,y) = {} & 0.331559 - 28.356y + 180.23y^2 - 291.345y^3 + 73.5919y^4 + 27.8101y^5 + 25.868x - 1.76231xy - 354.954xy^2 \\ & + 739.011xy^3 - 218.704xy^4 - 136.32x^2 + 132.505x^2y + 110.997x^2y^2 - 383.505x^2y^3 + 263.345x^3 - 178.352x^3y \\ & + 73.0549x^3y^2 - 226.043x^4 + 73.0559x^4y + 72.2912x^5.\end{aligned}$$

Polynomial of 6th order for the triangle representation of the ternary *n*-octane adsorption onto TA 95 at 298 K:

$$\begin{aligned}z(x,y) = {} & 0.253053 - 38.0541y + 429.896y^2 - 891.194y^3 + 817.17y^4 - 377.071y^5 + 74.7784y^6 + 36.5601x - 3.61847xy \\ & - 1658.56xy^2 + 2749.36xy^3 - 1809.51xy^4 + 451.716xy^5 - 260.608x^2 + 456.132x^2y + 2747.78x^2y^2 - 2743.68x^2y^3 \\ & + 837.755x^2y^4 + 785.183x^3 - 1332.84x^3y - 2248.25x^3y^2 + 977.566x^3y^3 - 1220.44x^4 + 1567.83x^4y + 712.294x^4y^2 \\ & + 949.045x^5 - 658.724x^5y - 290.635x^6\end{aligned}$$

Polynomial of 5th order for the quadratic Goworek representation of the ternary *n*-octane adsorption onto TA 95 at 298 K:

$$\begin{aligned}z(x,y) = {} & 0.422484 + 21.2702y - 105.266y^2 + 185.742y^3 - 143.492y^4 + 40.7156y^5 - 17.2139x - 12.0043xy + 82.0586xy^2 \\ & - 94.6481xy^3 + 40.7392xy^4 + 46.9852x^2 - 28.6611x^2y - 24.4224x^2y^2 - 2.40928x^2y^3 - 26.8431x^3 + 45.747x^3y \\ & + 18.2677x^3y^2 - 23.3643x^4 - 23.7454x^4y + 20.0864x^5.\end{aligned}$$

Polynomial of 6th order for the quadratic Goworek representatio of the ternary *n*-octane adsorption onto TA 95 at 298 K:

$$\begin{aligned}z(x,y) = {} & 0.323403 + 29.8478y - 190.015y^2 + 499.311y^3 - 683.398y^4 + 479.04y^5 - 135.769y^6 - 15.3963x - 49.9044xy \\ & + 251.967xy^2 - 405.388xy^3 + 293.248xy^4 - 74.9734xy^5 + 46.1833x^2 + 9.76924x^2y - 157.512x^2y^2 + 158.431x^2y^3 \\ & - 68.4967x^2y^4 - 35.9375x^3 + 48.2152x^3y + 37.2679x^3y^2 - 6.37552x^3y^3 - 6.08154x^4 - 41.7687x^4y - 3.26422x^4y^2 \\ & + 9.05916x^5 + 9.53006x^5y + 1.80436x^6.\end{aligned}$$

n-Hexadecane

Polynomial of 5th order for the triangle representation of the ternary *n*-hexadecane adsorption onto TA 95 at 298 K:

$$\begin{aligned}z(x,y) = {} & 0.768617 + 34.6848y - 842.647y^2 + 1594.82y^3 - 968.035y^4 + 182.596y^5 - 0.988871x + 155.327xy + 2096.12xy^2 \\ & - 3200.78xy^3 + 1068.7xy^4 - 10.0802x^2 - 659.653x^2y - 1615.16x^2y^2 + 1569.38x^2y^3 + 36.2503x^3 + 739.712x^3y \\ & + 346.144x^3y^2 - 45.6388x^4 - 262.736x^4y + 20.171x^5.\end{aligned}$$

Polynomial of 6th order for the triangle representation of the ternary *n*-hexadecane adsorption onto TA 95 at 298 K:

$$\begin{aligned}z(x,y) = {} & 0.641744 + 121.739y - 3773.44y^2 + 9068.81y^3 - 8345.55y^4 + 3492.53y^5 - 566.084y^6 - 5.19878x + 281.378xy \\ & + 15298.8xy^2 - 29809.6xy^3 + 18617.8xy^4 - 3894.59xy^5 + 32.978x^2 - 2858.23x^2y - 23059.2x^2y^2 + 32738.2x^2y^3 \\ & - 10390.2x^2y^4 - 145.372x^3 + 6073.37x^3y + 14960.5x^3y^2 - 11948.3x^3y^3 + 321.953x^4 - 5325.34x^4y - 3414.84x^4y^2 \\ & - 326.902x^5 + 1716.56x^5y + 122.529x^6.\end{aligned}$$

Polynomial of 5th order for the quadratic Goworek representation of the ternary *n*-hexadecane adsorption onto TA 95 at 298 K:

$$\begin{aligned}z(x,y) = {} & 0.750902 - 0.105122y - 6.68335y^2 + 16.9138y^3 - 21.0439y^4 + 10.6722y^5 + 19.0326x - 15.2856xy + 25.0483xy^2 \\ & - 25.3291xy^3 + 0.556487xy^4 - 95.4824x^2 + 64.4743x^2y - 4.65454x^2y^2 + 20.966x^2y^3 + 142.632x^3 - 96.4527x^3y \\ & - 16.6248x^3y^2 - 79.6268x^4 + 47.8738x^4y + 12.5955x^5.\end{aligned}$$

Polynomial of 6th order for the quadratic Goworek representation of the ternary *n*-hexadecane adsorption onto TA 95 at 298 K:

$$\begin{aligned}z(x,y) = {} & 0.819777 - 6.39357y + 56.8211y^2 - 236.218y^3 + 444.233y^4 - 368.116y^5 + 127.531y^6 + 21.569x + 44.1798xy \\ & - 128.302xy^2 + 113.526xy^3 - 70.9593xy^4 + 19.6782xy^5 - 248.807x^2 + 148.679x^2y + 218.782x^2y^2 - 136.292x^2y^3 \\ & + 26.9802x^2y^4 + 702.322x^3 - 706.122x^3y - 43.4115x^3y^2 + 50.6492x^3y^3 - 829.185x^4 + 782.589x^4y - 51.7635x^4y^2 \\ & + 427.466x^5 - 268.035x^5y - 74.1328x^6.\end{aligned}$$

---

interactions between n-hexadecane and carbon surface are stronger as a consequence of the higher dispersion forces of n-hexadecane. The relative open pore system of TA 95 (micropore diameter about 8 Å) permits coiled molecules like n-hexadecane to reach the surface. In the case of n-octane adsorption, the binary adsorption azeotrope of ethanol/n-octane at $x_{n\text{-octane}} \approx 0.62$ marks again the beginning of the ternary adsorption azeotrope, which is shifting in the ethanol rich direction with increasing of the n-hexadecane concentration. In the ethanol rich corner of the triangle near the ternary adsorption azeotrope, n-octane is preferentially adsorbed from ethanol, but at the same time n-hexadecane is preferentially adsorbed from n-octane and ethanol. The competition of n-hexadecane and n-octane molecules causes a shifting of the ternary azeotrope of n-octane in the ethanol rich direction, which is stronger than the shifting of the ternary azeotrope of ethanol. In the n-hexadecane rich area above the miscibility gap, n-octane is preferentially adsorbed by values about 0.1 or 0.2 mmol/g, too. This result is difficult to understand because it contains the paradox of a preferential adsorption of n-octane molecules from n-hexadecane (ethanol concentrations are very small) onto activated carbon. Furthermore, these small values about 0.1 or 0.2 mmol/g could be within the error interval of the adsorption excess because of the measurement difficulties in the area above the miscibility gap. Therefore, we want to refrain from a discussion.

n-Hexadecane (Fig. 11(b)) is preferentially adsorbed in the whole concentration range except the n-hexadecane rich area above the miscibility gap. The behaviour in this area again is influenced by the real characteristics of the bulk phase. The long-chain n-hexadecane disturbs the ethanol association and ethanol is enriched in the adsorption phase.

In the discussion of the ternary adsorption of ethanol/n-octane/n-hexadecane onto activated carbon TA 95, it is evident that the real characteristics of the bulk phase is an important factor influencing the quantity and the shape of the adsorption excess (compare factors and properties of the adsorbent and the adsorbate responsible for quantity and shape of the adsorption isotherms in (Myers, 1989)).

Cuttings through a polynomial surface with a Gibbs triangle basis allow a deeper understanding of the overlying ternary adsorption processes. In Fig. 12 the position of cuttings in the ternary triangle is marked.

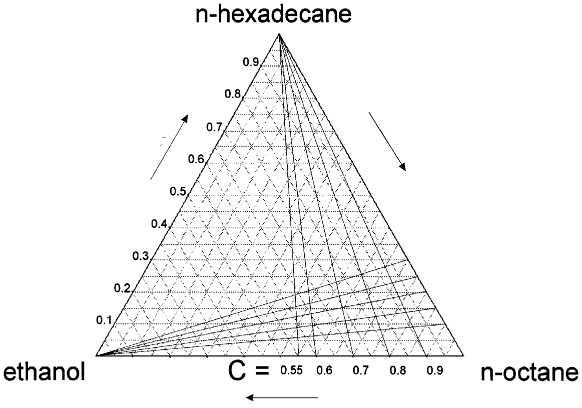

Figure 12. Cuttings of the polynomial surfaces $y = f(x_1, x_2, x_3)$.

In the first case, the pointed out component x_3 of ternary mixture is n-hexadecane. Thus the constant C is given by $x_{n\text{-octane}}/(x_{n\text{-octane}} + x_{\text{ethanol}})$. The cuttings of the three polynomial surfaces are illustrated in Figs. 13(a)–(c). In the second case, the pointed out component is ethanol. Thus the constant C is given by $x_{n\text{-hexadecane}}/(x_{n\text{-hexadecane}} + x_{n\text{-octane}})$. The cutting of the n-octane polynomial surface is shown in Fig. 14.

All cuttings are normalized to 1.

A comparison of the ternary adsorption of n-octane at 298 K (Fig. 13(a)) with the binary adsorption of n-octane at 298 K (Fig. 3) shows the development inside the ternary triangle. The maximal negative excess of n-octane from binary mixture is about -1 mmol/g, lying at $x_{n\text{-hexadecane}} \approx 0.4$. With an increase of the ethanol content in ternary mixture (decreasing from $C = 0.9$ to $C = 0.7$) the maximal negative excess is increasing to about -1.3 mmol/g and shifted to smaller mole fractions of n-hexadecane. The increasing of the negative excess in this concentration range is well-founded in an addition of adsorption effects. n-Hexadecane and ethanol are preferentially adsorbed from n-octane. At $C = 0.6$ the maximal negative excess of n-octane is decreasing. The turning point harmonizes with the adsorption azeotrope of the binary mixture ethanol/n-octane. Especially at the higher mole fraction of n-hexadecane the development is contrary. With an increase of C the negative excess of n-octane is stepwise decreasing. In this way the shape of the ternary isotherms moves step by step from the binary starting point.

The cuttings of the ternary adsorption of n-hexadecane are illustrated in Fig. 13(b) and show a similar behaviour, but with a reversed sign. In

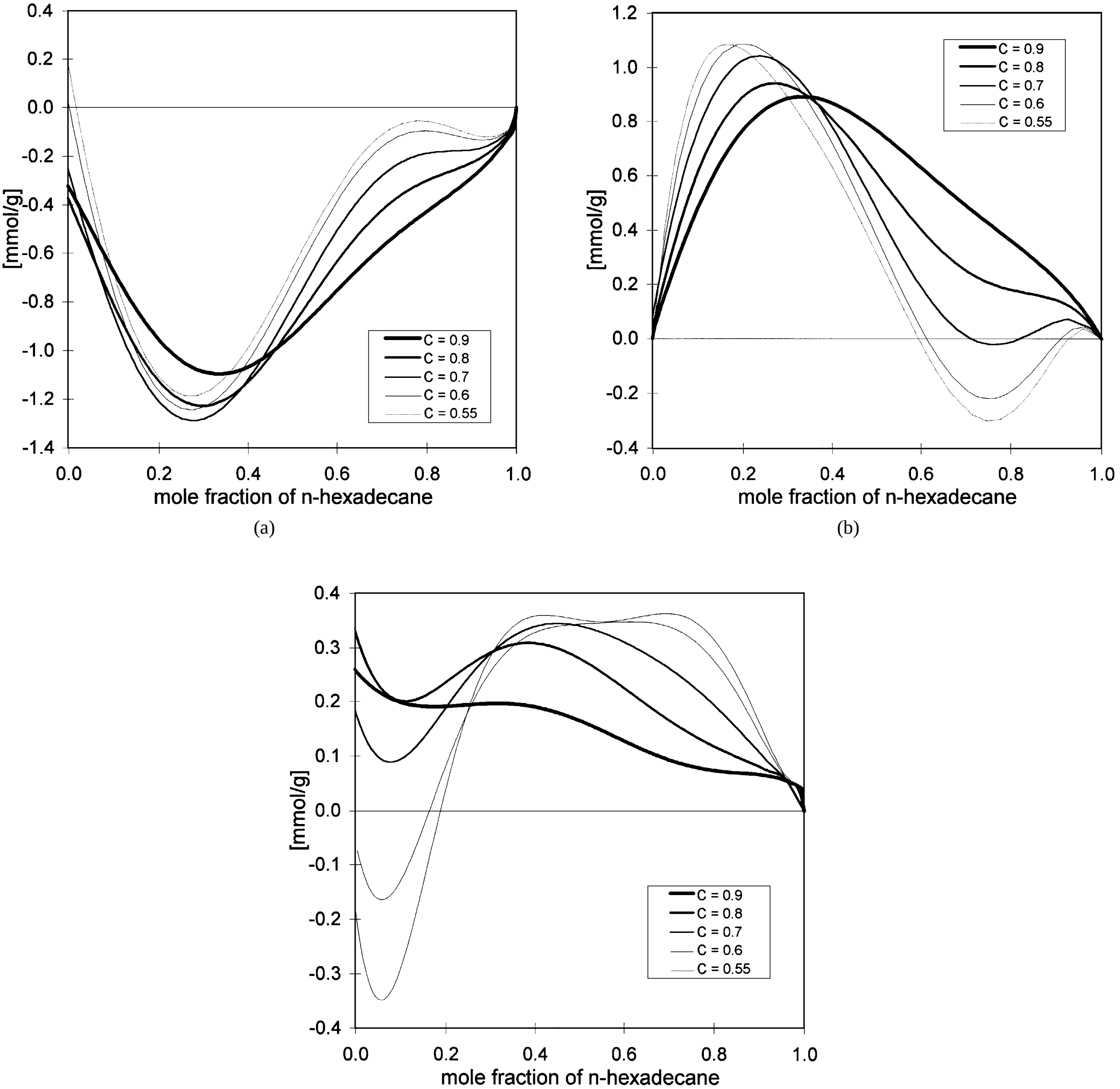

(a)

(b)

(c)

Figure 13. Cuttings of the polynomial surface: (a) $\Gamma^{\sigma}_{n\text{-octane}} = f(x_1, x_2, x_3)$, (b) $\Gamma^{\sigma}_{n\text{-hexadecane}} = f(x_1, x_2, x_3)$, (c) $\Gamma^{\sigma}_{\text{ethanol}} = f(x_1, x_2, x_3)$ for five different values C ($C = x_2/(x_2 + x_1)$, n-hexadecane is the pointed out component x_3).

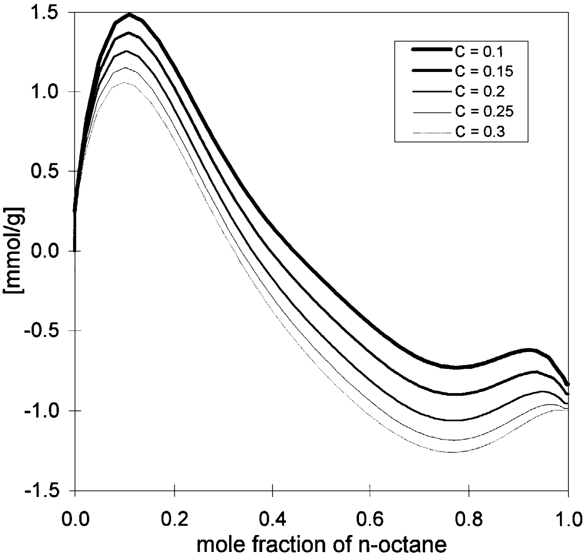

Figure 14. Cuttings of the polynomial surface $\Gamma^{\sigma}_{n\text{-octane}} = f(x_1, x_2, x_3)$ for five different values $C = x_3/(x_3 + x_2)$, ethanol is the pointed out component x_1.

difference to the n-octane adsorption an azeotrope appears at $C = 0.7$, which is growing with the decrease of C. The n-hexadecane rich area above the miscibility gap is reached, where ethanol is preferentially adsorbed as a result of the disturbed ethanol association.

The cuttings of the ethanol surface are shown in Fig. 13(c). A relative uniform positive adsorption is given at $C = 0.9$. With decreasing C from $= 0.9$ to 0.55 the adsorption excess of ethanol at $x_{n\text{-hexadecane}} \approx 0.1$ is diminishing. The change of sign harmonizes with the adsorption azeotrope of the binary mixture ethanol/n-octane. In the higher concentration range of n-hexadecane the adsorption excess of ethanol increases according to the disturbance of the associate formation.

At last the cuttings of the n-octane adsorption in the other direction of the ternary triangle are illustrated in Fig. 14. Comparing the ternary excess of n-octane with the binary excess shown in Fig. 2 the similarity is evident. With the increase of C the adsorption excess is decreasing step by step at $x_{\text{ethanol}} \approx 0.1$ and $x_{\text{ethanol}} \approx 0.8$ as a result of the increasing n-hexadecane competition.

Conclusions

A discussion of the ternary adsorption excess isotherms for the system ethanol/n-octane/n-hexadecane/TA 95 was possible with help of an intensive description of measured binary and ternary data. To determine the ternary adsorption excess on the binodal curve, a new approach was introduced. A mathematical description of ternary adsorption was given in the form $y = f(x_1, x_2, x_3)$ with the basis of a Gibbs triangle and the three-dimensional representation $y = f(x_3, C)$ after Goworek.

The interpolated polynomials are the basis for the calculations of the specific free wetting energy and thus for the whole thermodynamic treatment. The calculations of the ternary immersion quantities from ternary adsorption isotherms and activity coefficients are to be published in an intended paper (Bräuer et al., 1998).

Table 3. Experimental adsorption excess data for the system ethanol/n-octane n-hexadecane/TA 95 at 298 K.

	Mole fraction ethanol	Mole fraction n-octane	Mole fraction n-hexadecane	Excess ethanol [mmol/g]	Excess n-octane [mmol/g]	Excess n-hexadecane [mmol/g]
1	0.1513	0.0000	0.8487	0.3641	0.0000	−0.3641
2	0.1384	0.0000	0.8616	0.4413	0.0000	−0.4413
3	0.1251	0.0000	0.8749	0.3024	0.0000	−0.3024
4	0.1023	0.0000	0.8977	0.3241	0.0000	−0.3241
5	0.0882	0.0000	0.9118	0.2532	0.0000	−0.2532
6	0.0787	0.0000	0.9213	0.2586	0.0000	−0.2586
7	0.0690	0.0000	0.9310	0.2754	0.0000	−0.2754
8	0.0542	0.0000	0.9458	0.2319	0.0000	−0.2319
9	0.0185	0.0000	0.9815	0.1453	0.0000	−0.1453
10	0.0079	0.0000	0.9921	0.0843	0.0000	−0.0843
11	0.0404	0.9108	0.0487	0.2340	−0.5470	0.3130
12	0.0363	0.9141	0.0496	0.2359	−0.5454	0.3095
13	0.0397	0.8997	0.0605	0.2301	−0.6433	0.4132

(*Continued on next page*).

(*Continued*.)

	Mole fraction ethanol	Mole fraction *n*-octane	Mole fraction *n*-hexadecane	Excess ethanol [mmol/g]	Excess *n*-octane [mmol/g]	Excess *n*-hexadecane [mmol/g]
14	0.0362	0.8810	0.0827	0.2276	−0.7355	0.5079
15	0.0313	0.8377	0.1309	0.2012	−0.8222	0.6210
16	0.0291	0.8080	0.1629	0.1796	−0.8630	0.6834
17	0.0434	0.7440	0.2126	0.1621	−0.9264	0.7643
18	0.0256	0.6998	0.2746	0.1534	−1.0744	0.9210
19	0.0236	0.6610	0.3155	0.1587	−1.0999	0.9412
20	0.0227	0.6288	0.3486	0.1621	−1.0533	0.8912
21	0.0202	0.5844	0.3955	0.1432	−1.0645	0.9213
22	0.0147	0.5350	0.4503	0.1197	−1.0209	0.9012
23	0.0164	0.4848	0.4987	0.1107	−0.9671	0.8564
24	0.0121	0.4419	0.5461	0.1059	−0.9072	0.8013
25	0.0149	0.3795	0.6056	0.1076	−0.8508	0.7432
26	0.0132	0.3274	0.6594	0.1128	−0.6495	0.5367
27	0.0129	0.2663	0.7209	0.1136	−0.5256	0.4120
28	0.0118	0.2128	0.7754	0.1149	−0.4289	0.3140
29	0.0091	0.1559	0.8350	0.1150	−0.3306	0.2156
30	0.0161	0.1046	0.8793	0.1153	−0.3166	0.2013
31	0.0786	0.8854	0.0360	0.2205	−0.5717	0.3512
32	0.0880	0.8504	0.0617	0.2214	−0.5681	0.3467
33	0.0791	0.8259	0.0950	0.2203	−0.6559	0.4356
34	0.0803	0.8005	0.1192	0.2293	−0.7527	0.5234
35	0.0780	0.7822	0.1397	0.2178	−0.8165	0.5987
36	0.0757	0.7385	0.1858	0.2012	−0.9012	0.7000
37	0.0588	0.7012	0.2399	0.1998	−0.9630	0.7632
38	0.0686	0.6392	0.2923	0.1843	−1.1464	0.9621
39	0.0488	0.6008	0.3503	0.1897	−1.1209	0.9312
40	0.0412	0.5532	0.4055	0.1978	−1.1276	0.9298
41	0.0440	0.4646	0.4914	0.1903	−1.0726	0.8823
42	0.0451	0.4097	0.5451	0.1865	−0.9586	0.7721
43	0.0263	0.3605	0.6131	0.1756	−0.9010	0.7254
44	0.0234	0.2858	0.6907	0.1534	−0.8466	0.6932
45	0.0275	0.2289	0.7435	0.1476	−0.7174	0.5698
46	0.0186	0.1922	0.7891	0.1365	−0.5698	0.4333
47	0.0014	0.1420	0.8567	0.1305	−0.4492	0.3187
48	0.0013	0.0415	0.9572	0.1302	−0.3689	0.2387
49	0.0019	0.0383	0.9598	0.1087	−0.2958	0.1871
50	0.1360	0.8294	0.0346	0.2110	−0.5921	0.3811
51	0.1333	0.8291	0.0375	0.2128	−0.5949	0.3821
52	0.1306	0.8106	0.0589	0.2240	−0.6893	0.4653
53	0.1249	0.7979	0.0773	0.2350	−0.7830	0.5480
54	0.1138	0.7668	0.1194	0.2354	−0.8645	0.6291
55	0.0997	0.7330	0.1673	0.2328	−0.9347	0.7019
56	0.0938	0.6816	0.2246	0.2330	−0.9284	0.6954

(*Continued on next page*).

(*Continued*.)

	Mole fraction ethanol	Mole fraction *n*-octane	Mole fraction *n*-hexadecane	Excess ethanol [mmol/g]	Excess *n*-octane [mmol/g]	Excess *n*-hexadecane [mmol/g]
57	0.0941	0.6358	0.2701	0.2337	−0.9324	0.6987
58	0.0788	0.6056	0.3157	0.2398	−1.0611	0.8213
59	0.0667	0.5767	0.3565	0.2454	−1.1905	0.9451
60	0.0620	0.5394	0.3986	0.2581	−1.0798	0.8217
61	0.0654	0.4858	0.4487	0.2611	−0.9961	0.7350
62	0.0568	0.4436	0.4995	0.2354	−0.8678	0.6324
63	0.0480	0.8380	0.5640	0.2192	−0.7488	0.5296
64	0.0325	0.3183	0.6493	0.2045	−0.6301	0.4256
65	0.0330	0.2719	0.6950	0.1980	−0.5343	0.3363
66	0.0306	0.2310	0.7383	0.1834	−0.4012	0.2178
67	0.0271	0.1908	0.7821	0.1748	−0.3005	0.1257
68	0.0166	0.1522	0.8312	0.1034	−0.2346	0.1312
69	0.0210	0.1031	0.8759	0.0192	−0.1621	0.1429
70	0.1795	0.7843	0.0363	0.1734	−0.5732	0.3998
71	0.1736	0.7560	0.0703	0.1754	−0.5775	0.4021
72	0.1794	0.7396	0.0811	0.1790	−0.6794	0.5004
73	0.1724	0.7098	0.1179	0.1890	−0.7693	0.5803
74	0.1673	0.6879	0.1448	0.2034	−0.8789	0.6755
75	0.1564	0.6574	0.1861	0.2045	−0.9824	0.7779
76	0.1334	0.6334	0.2332	0.2043	−1.0253	0.8210
77	0.1315	0.5823	0.2861	0.2245	−1.0899	0.8654
78	0.1228	0.5536	0.3235	0.2298	−1.2230	0.9932
79	0.1209	0.5317	0.3473	0.2394	−1.3328	1.0934
80	0.1116	0.5120	0.3764	0.2599	−1.1833	0.9234
81	0.0999	0.4725	0.4276	0.2734	−1.0067	0.7333
82	0.0769	0.4291	0.4940	0.2534	−0.9083	0.6549
83	0.0785	0.4007	0.5208	0.2267	−0.7634	0.5367
84	0.0651	0.3687	0.5661	0.2245	−0.6474	0.4229
85	0.0652	0.3254	0.6095	0.2200	−0.5449	0.3249
86	0.0533	0.2863	0.6604	0.2104	−0.4108	0.2004
87	0.0439	0.2435	0.7127	0.1657	−0.2935	0.1278
88	0.0248	0.1672	0.8081	0.1231	−0.2333	0.1102
89	0.2314	0.7184	0.0502	0.1578	−0.5768	0.4190
90	0.2319	0.7307	0.0373	0.1505	−0.5769	0.4264
91	0.2242	0.7154	0.0604	0.1556	−0.7000	0.5444
92	0.2196	0.6974	0.0830	0.1615	−0.8005	0.6390
93	0.2139	0.6545	0.1315	0.1435	−0.8747	0.7312
94	0.2047	0.6302	0.1651	0.1252	−0.9687	0.8435
95	0.1883	0.6079	0.2038	0.1705	−1.1245	0.9540
96	0.1767	0.5813	0.2420	0.2117	−1.2972	1.0856
97	0.1543	0.5517	0.2940	0.2249	−1.4038	1.1789
98	0.1380	0.5217	0.3403	0.2360	−1.5009	1.2649

(*Continued on next page*).

(*Continued*.)

	Mole fraction ethanol	Mole fraction *n*-octane	Mole fraction *n*-hexadecane	Excess ethanol [mmol/g]	Excess *n*-octane [mmol/g]	Excess *n*-hexadecane [mmol/g]
99	0.1197	0.4709	0.4095	0.2649	−1.2673	1.0024
100	0.1130	0.4257	0.4613	0.2924	−1.0297	0.7372
101	0.1025	0.3755	0.5220	0.2678	−0.9469	0.6791
102	0.0902	0.3406	0.5692	0.2333	−0.7746	0.5414
103	0.0687	0.3007	0.6306	0.2756	−0.6987	0.4231
104	0.0540	0.2621	0.6840	0.3926	−0.7118	0.3192
105	0.0434	0.2148	0.7419	0.2834	−0.4835	0.2001
106	0.0326	0.1830	0.7843	0.1646	−0.3034	0.1388
107	0.0336	0.1336	0.8329	0.1434	−0.2346	0.0912
108	0.0162	0.0900	0.8937	0.1297	−0.2039	0.0742
109	0.2843	0.6867	0.0290	0.0523	−0.4087	0.3564
110	0.2828	0.6696	0.0476	0.0324	−0.4027	0.3703
111	0.2879	0.6481	0.0640	0.0723	−0.5944	0.5221
112	0.2886	0.6292	0.0822	0.0834	−0.7232	0.6398
113	0.2827	0.5917	0.1255	0.0945	−0.8543	0.7598
114	0.2649	0.5735	0.1617	0.1200	−1.0132	0.8932
115	0.2460	0.5458	0.2082	0.1567	−1.1468	0.9901
116	0.2228	0.5230	0.2543	0.2345	−1.3045	1.0700
117	0.2095	0.5119	0.2786	0.2419	−1.3222	1.0803
118	0.1811	0.4879	0.3311	0.2314	−1.3145	1.0831
119	0.1737	0.4543	0.3720	0.2512	−1.1504	0.8992
120	0.1548	0.4500	0.3953	0.2659	−0.9382	0.6723
121	0.1441	0.4197	0.4362	0.2435	−0.8334	0.5899
122	0.1344	0.3770	0.4886	0.2333	−0.7033	0.4700
123	0.1195	0.3405	0.5401	0.2413	−0.6206	0.3793
124	0.1022	0.3024	0.5954	0.2645	−0.5305	0.2660
125	0.0901	0.2511	0.6588	0.2314	−0.4070	0.1756
126	0.0710	0.2116	0.7174	0.1534	−0.2566	0.1032
127	0.0475	0.1585	0.7940	0.1300	−0.1832	0.0532
128	0.0269	0.0479	0.9251	0.1154	−0.1675	0.0521
129	0.3265	0.6489	0.0246	−0.1034	−0.1978	0.3012
130	0.3409	0.6308	0.0283	−0.1426	−0.2092	0.3519
131	0.3319	0.6321	0.0360	−0.0756	−0.4333	0.5089
132	0.3356	0.6058	0.0585	−0.0341	−0.6134	0.6475
133	0.3203	0.5809	0.0988	0.0034	−0.8144	0.8110
134	0.3213	0.5289	0.1498	0.0974	−1.0580	0.9606
135	0.2788	0.5278	0.1934	0.1478	−1.1823	1.0345
136	0.2506	0.4946	0.2548	0.2619	−1.3598	1.0979
137	0.2256	0.4676	0.3068	0.2545	−1.2758	1.0213
138	0.2090	0.4597	0.3312	0.2456	−1.1764	0.9308
139	0.1788	0.4118	0.4095	0.2435	−0.9975	0.7540
140	0.1536	0.3804	0.4660	0.2348	−0.8236	0.5888

(*Continued on next page*).

(*Continued*.)

	Mole fraction ethanol	Mole fraction *n*-octane	Mole fraction *n*-hexadecane	Excess ethanol [mmol/g]	Excess *n*-octane [mmol/g]	Excess *n*-hexadecane [mmol/g]
141	0.1445	0.3513	0.5043	0.2376	−0.7346	0.4970
142	0.1221	0.3096	0.5683	0.2460	−0.6380	0.3920
143	0.0947	0.2681	0.6373	0.2300	−0.5322	0.3022
144	0.0858	0.2288	0.6854	0.2269	−0.4334	0.2064
145	0.0597	0.1807	0.7596	0.1768	−0.3291	0.1523
146	0.0598	0.1519	0.7883	0.1412	−0.2121	0.0709
147	0.0464	0.1148	0.8389	0.1254	−0.1732	0.0478
148	0.0307	0.0769	0.8924	0.1008	−0.1284	0.0276
149	0.3852	0.5858	0.0290	−0.0945	−0.3321	0.4266
150	0.3650	0.5758	0.0592	−0.1123	−0.3548	0.4671
151	0.3654	0.5478	0.0867	−0.0699	−0.5488	0.6187
152	0.3457	0.5239	0.1304	−0.0213	−0.7598	0.7811
153	0.3350	0.5136	0.1515	−0.0121	−0.8881	0.9002
154	0.3169	0.4975	0.1856	0.0034	−1.0268	1.0234
155	0.2923	0.4731	0.2345	0.1465	−1.2077	1.0612
156	0.2732	0.4482	0.2786	0.3024	−1.4056	1.1032
157	0.2563	0.4187	0.3250	0.3214	−1.3253	1.0021
158	0.2176	0.3976	0.3847	0.3124	−1.2145	0.9021
159	0.2049	0.3833	0.4118	0.3512	−1.0122	0.6610
160	0.1819	0.3577	0.4604	0.3624	−0.8324	0.4700
161	0.1671	0.3071	0.5259	0.3012	−0.6911	0.3899
162	0.1531	0.2637	0.5831	0.2611	−0.5632	0.3021
163	0.1330	0.2434	0.6237	0.1823	−0.4521	0.2698
164	0.1619	0.1687	0.6695	0.1654	−0.3686	0.2032
165	0.0990	0.1836	0.7174	0.1032	−0.2356	0.1324
166	0.0778	0.1552	0.7670	0.1204	−0.1725	0.0521
167	0.0676	0.1166	0.8158	0.0932	−0.1443	0.0511
168	0.0545	0.0897	0.8559	0.0756	−0.0726	−0.0030
169	0.4313	0.5393	0.0293	−0.0856	−0.4576	0.5432
170	0.4293	0.5389	0.0318	−0.0996	−0.4494	0.5490
171	0.4151	0.5347	0.0502	−0.0642	−0.6571	0.7213
172	0.4043	0.5336	0.0620	0.0491	−0.9979	0.9488
173	0.3763	0.5115	0.1121	−0.0349	−1.0161	1.0510
174	0.3596	0.5012	0.1392	−0.0102	−1.1384	1.1486
175	0.3358	0.4768	0.1874	0.1467	−1.2791	1.1324
176	0.3089	0.4493	0.2417	0.3541	−1.4752	1.1211
177	0.2850	0.4224	0.2926	0.3710	−1.3733	1.0023
178	0.2614	0.3842	0.3544	0.3833	−1.2613	0.8780
179	0.2321	0.3611	0.4068	0.4536	−1.0034	0.5498
180	0.1937	0.3315	0.4748	0.4940	−0.8611	0.3672
181	0.2040	0.2814	0.5145	0.3768	−0.6769	0.3001
182	0.1924	0.2482	0.5594	0.2877	−0.5309	0.2432

(*Continued on next page*).

(*Continued*.)

	Mole fraction ethanol	Mole fraction *n*-octane	Mole fraction *n*-hexadecane	Excess ethanol [mmol/g]	Excess *n*-octane [mmol/g]	Excess *n*-hexadecane [mmol/g]
183	0.1504	0.2102	0.6394	0.1376	−0.3625	0.2249
184	0.1302	0.1924	0.6774	0.0998	−0.3065	0.2066
185	0.1023	0.1575	0.7402	0.0143	−0.1066	0.0923
186	0.0798	0.1298	0.7904	0.1195	−0.1553	0.0358
187	0.0794	0.1200	0.8007	0.0769	−0.1412	0.0643
188	0.0442	0.0662	0.8895	0.0485	−0.1422	0.0937
189	0.0198	0.0389	0.9413	0.0577	−0.0518	−0.0060
190	0.0385	0.0583	0.9032	0.1365	−0.0778	−0.0587
191	0.0539	0.0937	0.8523	0.2049	−0.1436	−0.0613
192	0.0664	0.1270	0.8066	0.2854	−0.1964	−0.0889
193	0.1010	0.1543	0.7447	0.2715	−0.2431	−0.0284
194	0.1257	0.1764	0.6979	0.2690	−0.2847	0.0157
195	0.1532	0.2247	0.6221	0.2491	−0.4784	0.2293
196	0.1399	0.2458	0.6142	0.4909	−0.2617	−0.2292
197	0.2000	0.2724	0.5276	0.3062	−0.5686	0.2624
198	0.2481	0.2917	0.4602	0.0730	−0.5462	0.4732
199	0.0601	0.0314	0.9085	0.2464	−0.0503	−0.1961
200	0.0721	0.0693	0.8586	0.3419	−0.0998	−0.2421
201	0.1068	0.0934	0.7998	0.2720	−0.1670	−0.1050
202	0.1244	0.1122	0.7634	0.3872	−0.1920	−0.1952
203	0.1432	0.1395	0.7173	0.4277	−0.2146	−0.2132
204	0.1912	0.1655	0.6433	0.3195	−0.3301	0.0106
205	0.1878	0.2033	0.6089	0.5976	−0.4390	−0.1586
206	0.2411	0.2256	0.5333	0.2178	−0.4998	0.2820
207	0.0838	0.0374	0.8789	0.5179	−0.1512	−0.3667
208	0.1267	0.0579	0.8154	0.2995	−0.1000	−0.1995
209	0.1249	0.0924	0.7827	0.4372	0.0384	−0.4756
210	0.1300	0.1160	0.7540	0.5123	0.1377	−0.6500
211	0.1446	0.1510	0.7044	0.4966	0.2134	−0.7100
212	0.1417	0.1833	0.6751	0.6751	−0.2541	−0.4210
213	0.1227	0.0354	0.8419	0.7012	−0.0957	−0.6055
214	0.1345	0.0645	0.8010	0.5451	0.1791	−0.7242
215	0.1490	0.0947	0.7563	0.5501	0.2887	−0.8389
216	0.1460	0.0370	0.8170	0.7043	0.2810	−0.9853
217	0.9751	0.0246	0.0003	−3.4048	2.2213	1.1835
218	0.9945	0.0051	0.0004	−1.9622	0.7264	0.2359
219	0.5059	0.4678	0.0263	−1.0259	0.3120	0.7139
220	0.5260	0.4441	0.0300	−0.7168	0.1590	0.5577
221	0.5446	0.4255	0.0299	−0.7820	0.1146	0.6674
222	0.6193	0.3567	0.0240	−1.4669	0.6572	0.8097
223	0.6632	0.3128	0.0239	−2.0663	1.1992	0.8670

(*Continued on next page*).

(*Continued*.)

	Mole fraction ethanol	Mole fraction *n*-octane	Mole fraction *n*-hexadecane	Excess ethanol [mmol/g]	Excess *n*-octane [mmol/g]	Excess *n*-hexadecane [mmol/g]
224	0.6896	0.2877	0.0228	−1.7378	0.9205	0.8173
225	0.7151	0.2670	0.0179	−2.0162	0.9941	1.0221
226	0.7660	0.2241	0.0099	−2.8223	1.5019	1.3204
227	0.8063	0.1877	0.0059	−3.2579	1.8885	1.3695
228	0.7887	0.1990	0.0123	−2.6515	1.2607	1.3908
229	0.8387	0.1541	0.0072	−3.1866	1.6719	1.5146
230	0.8616	0.1296	0.0088	−2.9901	1.4771	1.5130
231	0.8546	0.1279	0.0175	−2.9236	1.2142	1.7094
232	0.9390	0.0558	0.0052	−3.5105	1.7110	1.7995
233	0.9806	0.0176	0.0018	−3.0996	1.2265	1.8732
234	0.9772	0.0170	0.0058	−3.0055	2.2645	0.7410
235	0.4776	0.4603	0.0621	−0.6552	−0.3295	0.9846
236	0.5108	0.4276	0.0615	−0.8962	−0.0918	0.9880
237	0.5261	0.3974	0.0765	−0.9879	−0.0270	1.0149
238	0.6028	0.3448	0.0524	−1.3143	0.0102	1.3041
239	0.6113	0.3227	0.0660	−1.4164	0.2064	1.2099
240	0.6466	0.2951	0.0583	−1.4834	0.1092	1.3742
241	0.6756	0.2653	0.0591	−1.9870	0.1030	1.8840
242	0.7374	0.2231	0.0395	−2.7247	0.8756	1.8492
243	0.7811	0.1805	0.0384	−2.3740	0.5366	1.8374
244	0.4223	0.4666	0.1111	−0.1788	−0.7599	0.9386
245	0.4883	0.4171	0.0946	−0.9854	−0.4191	1.4044
246	0.5064	0.3813	0.1123	−0.6064	−0.4652	1.0717
247	0.3556	0.4903	0.1542	−0.2302	−0.8273	1.0575
248	0.6115	0.2798	0.1088	−1.3108	−0.4738	1.7846
249	0.4210	0.4338	0.1452	−0.4739	−0.8385	1.3123
250	0.4552	0.4022	0.1426	−0.5474	−0.7392	1.2866
251	0.4688	0.3744	0.1568	−0.5081	−0.6288	1.1369
252	0.4219	0.3876	0.1905	−0.5450	−0.8528	1.3978
253	0.5603	0.3355	0.1042	−0.7561	−0.4569	1.2130
254	0.5065	0.3491	0.1443	−0.5213	−0.5967	1.1180
255	0.4535	0.4941	0.0523	−0.1865	−0.4255	0.6120
256	0.3775	0.4375	0.1850	−0.0213	−1.0107	1.0320
257	0.3462	0.4078	0.2461	0.1238	−1.1558	1.0320
258	0.2676	0.3500	0.3823	0.3214	−0.9334	0.6120
259	0.2204	0.1828	0.5969	0.4250	−0.2250	−0.2000
260	0.1812	0.1376	0.6812	0.5320	0.0890	−0.6210
261	0.2158	0.1158	0.6683	0.5210	0.0900	−0.6110
262	0.1786	0.0590	0.7624	0.3854	0.5356	−0.9210
263	0.2343	0.0589	0.7068	0.3743	0.0769	−0.4512
264	0.1894	0.0898	0.7209	0.3524	0.3908	−0.7432
265	1.0000	0.0000	0.0000	0.0000	0.0000	0.0000

(*Continued on next page*).

(*Continued.*)

	Mole fraction ethanol	Mole fraction *n*-octane	Mole fraction *n*-hexadecane	Excess ethanol [mmol/g]	Excess *n*-octane [mmol/g]	Excess *n*-hexadecane [mmol/g]
266	0.9868	0.0132	0.0000	−0.4470	0.4470	0.0000
267	0.9774	0.0226	0.0000	−0.7730	0.7730	0.0000
268	0.9619	0.0381	0.0000	−1.4000	1.4000	0.0000
269	0.9412	0.0588	0.0000	−1.1700	1.1700	0.0000
270	0.9267	0.0733	0.0000	−1.5000	1.5000	0.0000
271	0.8980	0.1020	0.0000	−2.1300	2.1300	0.0000
272	0.8635	0.1365	0.0000	−1.8300	1.8300	0.0000
273	0.8539	0.1461	0.0000	−2.0200	2.0200	0.0000
274	0.8264	0.1736	0.0000	−1.7500	1.7500	0.0000
275	0.7840	0.2160	0.0000	−1.7400	1.7400	0.0000
276	0.7524	0.2476	0.0000	−1.4000	1.4000	0.0000
277	0.7408	0.2592	0.0000	−1.7100	1.7100	0.0000
278	0.7023	0.2977	0.0000	−1.0400	1.0400	0.0000
279	0.6589	0.3411	0.0000	−0.9190	0.9190	0.0000
280	0.5700	0.4300	0.0000	−0.4980	0.4980	0.0000
281	0.5503	0.4497	0.0000	−0.4490	0.4490	0.0000
282	0.5135	0.4865	0.0000	−0.2440	0.2440	0.0000
283	0.4823	0.5177	0.0000	−0.3710	0.3710	0.0000
284	0.4466	0.5534	0.0000	−0.4060	0.4060	0.0000
285	0.4431	0.5569	0.0000	−0.1210	0.1210	0.0000
286	0.4062	0.5938	0.0000	−0.1330	0.1330	0.0000
287	0.3904	0.6069	0.0000	0.0000	0.0000	0.0000
288	0.3606	0.6394	0.0000	0.0000	0.0000	0.0000
289	0.3517	0.6483	0.0000	−0.1350	0.1350	0.0000
290	0.3114	0.6886	0.0000	0.2610	−0.2610	0.0000
291	0.2899	0.7101	0.0000	0.5200	−0.5200	0.0000
292	0.2684	0.7316	0.0000	0.2620	−0.2620	0.0000
293	0.2555	0.7445	0.0000	0.4060	−0.4060	0.0000
294	0.2255	0.7745	0.0000	0.1370	−0.1370	0.0000
295	0.1748	0.8252	0.0000	0.5350	−0.5350	0.0000
296	0.1365	0.8635	0.0000	0.4520	−0.4520	0.0000
297	0.0994	0.9006	0.0000	0.1110	−0.1110	0.0000
298	0.0928	0.9072	0.0000	0.1140	−0.1140	0.0000
299	0.9984	0.0000	0.0016	−0.2070	0.0000	0.2070
300	0.9982	0.0000	0.0018	−0.4730	0.0000	0.4730
301	0.9980	0.0000	0.0020	−0.6130	0.0000	0.6130
302	0.9980	0.0000	0.0020	−0.9260	0.0000	0.9260
303	0.9976	0.0000	0.0024	−1.1330	0.0000	1.1330
304	0.9958	0.0000	0.0042	−1.2660	0.0000	1.2660
305	0.9956	0.0000	0.0044	−1.3490	0.0000	1.3490
306	0.9943	0.0000	0.0057	−1.4350	0.0000	1.4350
307	0.9938	0.0000	0.0062	−1.3730	0.0000	1.3730
308	0.9895	0.0000	0.0105	−1.5860	0.0000	1.5860

(*Continued on next page*).

(*Continued*.)

	Mole fraction ethanol	Mole fraction *n*-octane	Mole fraction *n*-hexadecane	Excess ethanol [mmol/g]	Excess *n*-octane [mmol/g]	Excess *n*-hexadecane [mmol/g]
309	0.9610	0.0000	0.0390			
310	0.9520	0.0060	0.0420	−1.2314	0.3240	0.9074
311	0.8980	0.0490	0.0530	−1.8881	0.7543	1.1338
312	0.8700	0.0710	0.0600	−2.1000	0.7300	1.3700
313	0.8390	0.0960	0.0650	−1.7210	0.7899	0.9311
314	0.8070	0.1180	0.0740	−1.5430	0.6430	0.9000
315	0.6960	0.2120	0.0920	−1.6992	0.3120	1.3872
316	0.7320	0.1750	0.0940	−1.5432	0.5460	0.9972
317	0.7100	0.1950	0.0960	−2.0021	0.4120	1.5901
318	0.3660	0.3550	0.2790	0.6432	−1.3420	0.6988
319	0.3380	0.3690	0.2940	0.6623	−1.3651	0.7028
320	0.3160	0.3550	0.3290	0.5342	−1.2452	0.7110
321	0.2740	0.3140	0.4120	0.5987	−0.5002	−0.0985
322	0.2640	0.2440	0.4870	0.6129	−0.6210	0.0081
323	0.2620	0.2200	0.5180	0.5210	−0.4210	−0.1000
324	0.2620	0.1940	0.5440	0.4138	−0.3251	−0.0887
325	0.2650	0.0870	0.6480	0.4238	−0.4313	0.0075
326	0.2690	0.0000	0.7310			
327	0.0000	0.9967	0.0033	0.0000	−0.5830	0.5830
328	0.0000	0.9842	0.0158	0.0000	−0.7870	0.7870
329	0.0000	0.9294	0.0706	0.0000	−0.8690	0.8690
330	0.0000	0.8958	0.1042	0.0000	−0.8600	0.8600
331	0.0000	0.8781	0.1219	0.0000	−0.8900	0.8900
332	0.0000	0.8621	0.1379	0.0000	−0.8390	0.8390
333	0.0000	0.8428	0.1572	0.0000	−0.8930	0.8930
334	0.0000	0.8358	0.1642	0.0000	−0.8910	0.8910
335	0.0000	0.8131	0.1869	0.0000	−0.8140	0.8140
336	0.0000	0.7949	0.2051	0.0000	−0.9970	0.9970
337	0.0000	0.7831	0.2169	0.0000	−1.0000	1.0000
338	0.0000	0.7557	0.2443	0.0000	−0.9100	0.9100
339	0.0000	0.7498	0.2502	0.0000	−1.1000	1.1000
340	0.0000	0.7254	0.2746	0.0000	−1.0400	1.0400
341	0.0000	0.6931	0.3069	0.0000	−0.9530	0.9530
342	0.0000	0.6886	0.3114	0.0000	−1.0000	1.0000
343	0.0000	0.6584	0.3416	0.0000	−1.0000	0.0000
344	0.0000	0.6444	0.3556	0.0000	−0.9500	0.9500
345	0.0000	0.6034	0.3966	0.0000	−1.0500	0.0500
346	0.0000	0.5965	0.4035	0.0000	−0.9670	0.9670
347	0.0000	0.5750	0.4250	0.0000	−0.9670	0.9670
348	0.0000	0.5551	0.4449	0.0000	−0.9540	0.9540
349	0.0000	0.5409	0.4591	0.0000	−0.9440	0.9440
350	0.0000	0.5108	0.4892	0.0000	−0.9320	0.9320
351	0.0000	0.4927	0.5073	0.0000	−0.7220	0.7220

(*Continued on next page*).

(*Continued*.)

	Mole fraction ethanol	Mole fraction *n*-octane	Mole fraction *n*-hexadecane	Excess ethanol [mmol/g]	Excess *n*-octane [mmol/g]	Excess *n*-hexadecane [mmol/g]
352	0.0000	0.4778	0.5222	0.0000	−0.7720	0.7720
353	0.0000	0.4474	0.5526	0.0000	−0.6760	0.6760
354	0.0000	0.4339	0.5661	0.0000	−0.9120	0.9120
355	0.0000	0.4201	0.5799	0.0000	−0.9570	0.9570
356	0.0000	0.3656	0.6344	0.0000	−0.7750	0.7750
357	0.0000	0.3299	0.6701	0.0000	−0.8260	0.8260
358	0.0000	0.3140	0.6860	0.0000	−0.8010	0.8010
359	0.0000	0.2895	0.7105	0.0000	−0.6420	0.6420
360	0.0000	0.2790	0.7210	0.0000	−0.8620	0.8620
361	0.0000	0.2462	0.7538	0.0000	−0.8190	0.8190
362	0.0000	0.2240	0.7760	0.0000	−0.8950	0.8950
363	0.0000	0.1680	0.8320	0.0000	−0.5280	0.5280
364	0.0000	0.1491	0.8509	0.0000	−0.6070	0.6070
365	0.0000	0.1116	0.8884	0.0000	−0.6960	0.6960

Acknowledgments

The authors express their sincere appreciation to the Deutsche Forschungsgemeinschaft for the financial support (Qu 68/3-1). Also we wish to thank the Graduate College, “Physical Chemistry of Interfaces” at the University of Leipzig for being a source of encouragemens and help. For some measurements of the binary adsorption we thank C. Weiser. Last not least we acknowledge the financial support of the Fond der Chemischen Industrie.

References

Borowko, M. and W. Rzysko, *J. Colloid Interface Sci.*, **175**, 173 (1995).

Bräuer, P., M. Heuchel, T. Kind, M. Szombathely, U. Messow, B. Kind, and M. Jaroniec, *Chem. Technik*, **45**(1) (1993).

Bräuer, P., U. Messow, and G. Kalies, “The Adsorption of the Ternary Liquid Mixture Ethanol/*n*-Octane/*n*-Hexadecane onto Activated Carbon,” Part II (1998) (to be published).

Dahlmann, U. and G.M. Schneider, *J. Chem. Thermodynamics*, **21**, 997 (1989).

Everett, D.H., *Progr. Colloid and Polymer Sci.*, **65**, 103 (1978).

Findenegg, G.H., *J. Colloid Interface Sci.*, **35**, 249 (1971).

Forsythe, G., M. Malcolm, and C. Moler, *Computer Methods for Mathematical Computations*, p. 129, Prentice-Hall, Englewood Cliffs, 1977.

Gibbs, W.J., *Collected Works*, vol. 1, New York, 1931.

Goworek, J., *J. Colloid Interface Sci.*, **144**, 521 (1991).

Goworek, J., J. Oscik, and R. Kusak, *J. Colloid Interface Sci.*, **103**(2), 392 (1985).

Goworek, J. and R. Kusak, *Colloid Polym. Sci.*, **267**, 539 (1989).

Groszek, J., *Proc. R. Soc. London, Ser. A*, **314**, 473 (1970).

Heuchel, M., P. Bräuer, U. Messow, and M. Jaroniec, *Chemica Scripta*, **29**, 353 (1989).

Heuchel, M., P. Bräuer, and Z. Wiss, Karl-Marx-Univ., Leipzig, *Math.-Naturwiss. R.*, **35**, 401 (1986).

Jaroniec, M. and R. Madey, *Physical Adsorption on Heterogeneous Solids*, Elsevier, Amsterdam, 1988.

Kalies, G., U. Messow, and P. Bräuer, *Zeitschrift für Physikalische Chemie*, **191**, 87 (1995).

Kalies, G., G. Fleischer, M. Appel, U. Messow and J. Kärger, “Time-Dependence of the Adsorption of Ethanol/*n*-Octane onto Carbonaceous Adsorbents”, (1997) (to be published in Chem. Techn.).

Kern, H.E. and G.H. Findenegg, *J. Colloid Interface Sci.*, **75**, 346 (1980).

Messow, U., P. Bräuer, M. Heuchel, and M. Pysz, *Chem. Technik*, **44**(2), 56 (1992).

Mikhail, R.S., S. Brunauer, and E.E. Bodor, *J. Colloid Interface Sci.*, **26**, 45 (1968).

Moros, R. and H. Kalies, *CLB Chemie in Labor und Biotechnik*, **42**(9), 528 (1992).

Moros, R., H. Kalies, H.G. Rex, and S. Schaffarczyk, *Computers Chem. Engng.*, **20**(10), 1257 (1996).

Myers, A.L., *Proceedings of the Third Int. Conf. on Fundamentals of Adsorption*, Sonthofen, Germany, 1989.

Ozawa, S., K. Kawahara, M. Yamabe, H. Unno, and Y. Ogino, *J. Chem. Soc. Faraday Trans*, **80**, 1059 (1984).

Reuter, E. Diploma dissertation, University of Leipzig, 1995.

Saris, P., J.B. Rosenholm, E. Sjöblom, and U. Henriksson, *J. Phys. Chem.*, **90**, 660 (1986).

Surfer for Windows, Copyright Golden Software, Inc., 1994.